J Mater Sci (2011) 46:6871–6876
DOI 10.1007/s10853-011-5650-1

Construction of new morphotropic phase boundary in $0.94(K_{0.4-x}Na_{0.6}Ba_xNb_{1-x}Zr_x)O_3$–$0.06LiSbO_3$ lead-free piezoelectric ceramics

Wenfeng Liang · Wenjuan Wu · Dingquan Xiao · Jianguo Zhu · Jiagang Wu

Received: 22 March 2011 / Accepted: 19 May 2011 / Published online: 4 June 2011

Abstract $0.94(K_{0.4-x}Na_{0.6}Ba_xNb_{1-x}Zr_x)O_3$–$0.06LiSbO_3$ ceramics were prepared by conventional technique, and the effect of $BaZrO_3$ on the phase transitions, dielectric, ferroelectric, and piezoelectric properties of the ceramics were investigated. The phase transitions for the ceramics were determined by the temperature dependence of dielectric properties and X-ray diffraction patterns. $BaZrO_3$ changes the symmetry of the ceramics from tetragonal dominant phase with $x = 0$–0.06 to rhombohedral phase with $x = 0.07$–0.09. The phase transition near room temperature for the composition with $x \sim 0.06$ is different from previously reported phase transition between orthorhombic and tetragonal phases. It is suggested that a new morphotropic phase boundary (MPB) is constructed with both rhombohedral–orthorhombic and orthorhombic–tetragonal phase transitions near room temperature, and the enhanced piezoelectric properties ($d_{33} = 344$ pC/N and $k_P = 32.4\%$ with $x = 0.06$) are obtained. The results indicate that the construction of new MPB is of significance for further development of KNN-based ceramics.

Introduction

Environmental friendly non-toxic lead-free piezoelectric ceramics are investigated [1–21] for the purpose of replacing the widely used Pb(Zr, Ti)O_3 (PZT) materials. Especially, the (K, Na)NbO_3 (KNN)-based system has attracted extensive attention due to its' high piezoelectric properties and curie temperature (T_C) since the breakthrough obtained by Saito et al. [1]. However, most of the researchers are concentrated on modifying the orthorhombic–tetragonal transition temperature (T_{O-T}) down to around room temperature, and the properties obtained are still inferior compared to PZT system. Until very recently, the awkward situation for lead-free materials was changed by construction of morphotropic phase boundary (MPB) in $BaTiO_3$-based ceramics [21], and the piezoelectric properties ($d_{33} = 620$ pC/N) are comparable to corresponding lead-based piezoelectric ceramics. It should be noticed that the rather high sintering temperature and low T_C of the $BaTiO_3$-based ceramics still strongly restrict their applications, and the design of similar MPB in KNN-based system is not well studied yet.

For the lead-based ceramics, the MPB is generally associated with the narrow composition region between rhombohedral and tetragonal ferroelectric phases [22]. In order to get similar MPB in KNN lead-free piezoelectric ceramics, both the rhombohedral–orthorhombic transition temperature (T_{R-O}) and the orthorhombic–tetragonal transition temperature (T_{O-T}) of the ceramics should be modified to be near room temperature. It was reported that $BaZrO_3$ is effective to shift the T_{R-O} of KNN ceramics to be above room temperature [15]. As to T_{O-T}, it is widely investigated for the KNN-based ceramics by substitutions with $LiNbO_3$, $LiSbO_3$, $LiTaO_3$, $Bi_{0.5}Na_{0.5}TiO_3$, and $BaTiO_3$ etc. [5–14, 16, 19]. Among them, $LiSbO_3$-modified KNN-based ceramics with no expensive element draw quite a lot attention.

The basic objective of this study is to construct the new MPB in $0.94(K_{0.4-x}Na_{0.6}Ba_xNb_{1-x}Zr_x)O_3$–$0.06LiSbO_3$ lead-free piezoelectric ceramics and to investigate the effect of MPB on the electrical properties of the materials, in which the fundamental ceramics composition of $0.94K_{0.4}Na_{0.6}NbO_3$–$0.06LiSbO_3$ selected here is for

W. Liang · W. Wu · D. Xiao (✉) · J. Zhu · J. Wu
Department of Materials Science, Sichuan University, Chengdu 610064, China
e-mail: nic0402@scu.edu.cn

getting T_{O-T} near room temperature [16], and the further adjustment of the phase transition of the ceramics with $BaZrO_3$ is to increase the T_{R-O} of the ceramics to be around room temperature.

Experimental

The $0.94(K_{0.4-x}Na_{0.6}Ba_xNb_{1-x}Zr_x)O_3$–$0.06LiSbO_3$ ceramics were prepared by the conventional solid state reaction method with analytical-grade metal oxide and carbonate as raw materials: K_2CO_3 (99%), Na_2CO_3 (99.8%), Li_2CO_3 (98%), $BaCO_3$ (99%), Nb_2O_5 (99.5%), Sb_2O_3 (98%), and ZrO_2 (99%). The composition $BaZrO_3$ was first calcined at 1300 °C for 4 h, and then the calcined powder was mixed with other raw materials according to the composition. After ball milled for 24 h in ethanol, the mixed powders were dried and calcined at 850 °C for 6 h again. Subsequently, the calcined powders were milled again for 24 h, dried, and then pressed into disk samples with a diameter of 10 mm and thickness of 1 mm at 10 MPa using polyvinyl alcohol (PVA) as a binder. After burning off PVA, the samples were sintered at 1050–1140 °C for 2-3 h.

The crystalline structure of the ceramics was determined by X-ray diffraction (XRD) using Cu $K\alpha$ radiation ($\lambda = 1.54178$ Å) in the θ–2θ scan mode (DX1000, Dandong, China). Silver slurry was coated on both sides of the disks and then fired at 700 °C for 10 min to form electrodes for electrical measurements. The specimens were poled in silicon oil bath at room temperature under a DC electric field of 3-4 kV/mm for 20 min. The piezoelectric constant was measured using a piezo-d_{33} meter (ZJ-3A, China). The temperature dependence of dielectric constant was obtained using an LCR meter (Agilent 4980A, USA.). The hysteresis loops of the ceramics were measured using a Radiant Precision Workstation (USA) at 10 Hz.

Results and discussion

Figure 1a shows the XRD patterns in the range of 2θ from 20° to 60° for the $0.94(K_{0.4-x}Na_{0.6}Ba_xNb_{1-x}Zr_x)O_3$–$0.06LiSbO_3$ ceramics, and all of the patterns show pure perovskite structure except these compositions, with $x = 0.05$–0.09, have a secondary phase $K_3LiNb_6O_{17}$ according to JCPDS card NO. 36-0533. It can be observed that tetragonal dominant phase is obtained for the samples with $x = 0$–0.04 as shown in Fig. 1b (The corresponding XRD patterns are indexed by JCPDS card NO. 71-0945). It is noticeable that the two peaks around 46° for the samples shift to lower angle with the increase of x indicating cell volume extension owing to the diffusing of $BaZrO_3$ into the lattice to form a solid solution. Especially, the two

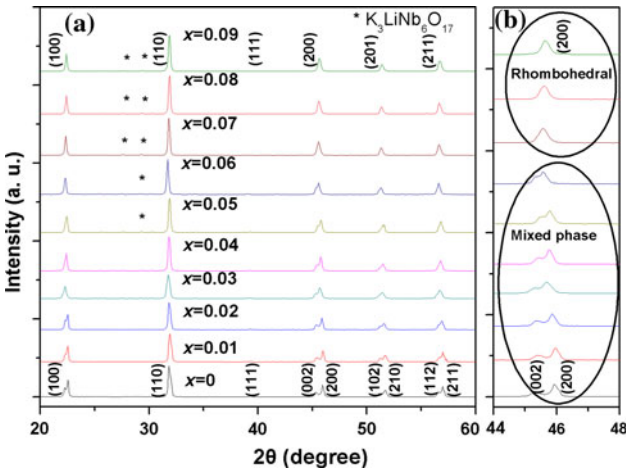

Fig. 1 The XRD patterns of the $0.94(K_{0.4-x}Na_{0.6}Ba_xNb_{1-x}Zr_x)O_3$–$0.06LiSbO_3$ ceramics in the 2θ range of **a** 20°–60° and **b** 44°–48°, respectively

peaks for compositions near $x = 0.05$ change suddenly indicating the existence of a phase boundary. Moreover, the peak split becomes more and more weak with the increase of x, and finally only one single peak is observed for the samples with $x = 0.07$–0.09 (The corresponding XRD patterns are indexed by JCPDS card NO. 71-0947) indicating the lattice parameters changed to be the same value. The single peak is a character for either rhombohedral or cubic phase [15], thus the dielectric and ferroelectric behavior are necessary in addition to XRD patterns to determine the symmetry of the ceramics with $x = 0.07$–0.09.

The temperature dependence of the dielectric constant (ε_r) at 10 kHz for the ceramics is shown in Fig 2a. The dielectric peak corresponding to T_C is clearly observed for the compositions with $x = 0.07$–0.09. The result together with the XRD analysis suggests that the symmetry of the ceramics should be rhombohedral phase at room temperature. The conclusion is in consistent with the phase diagram for KNN–$BaZrO_3$ system [15]. As shown in Fig. 2b, the addition of $BaZrO_3$ to the ceramics leads to the formation of two different dielectric anomalies related to the ferroelectric–ferroelectric phase transition near room temperature, one is the peak-like dielectric anomaly for the samples with $x = 0$–0.05, which is generally related to T_{O-T} and can be observed for most of the modified KNN-based ceramics [5–14, 16, 19], and the other one is a step-like dielectric anomaly for the samples with $x = 0.06$ and 0.07, and the ε_r of which increases with the increase of temperature until T_C. The appearance of step-like dielectric anomaly is generally accompanied with the increase of T_{R-O} in KNN-based ceramics as the situation for $BaZrO_3$ [15], or Sb^{5+} [17]-modified KNN ceramics. Moreover, it can be found that only one dielectric anomaly is observed for the composition

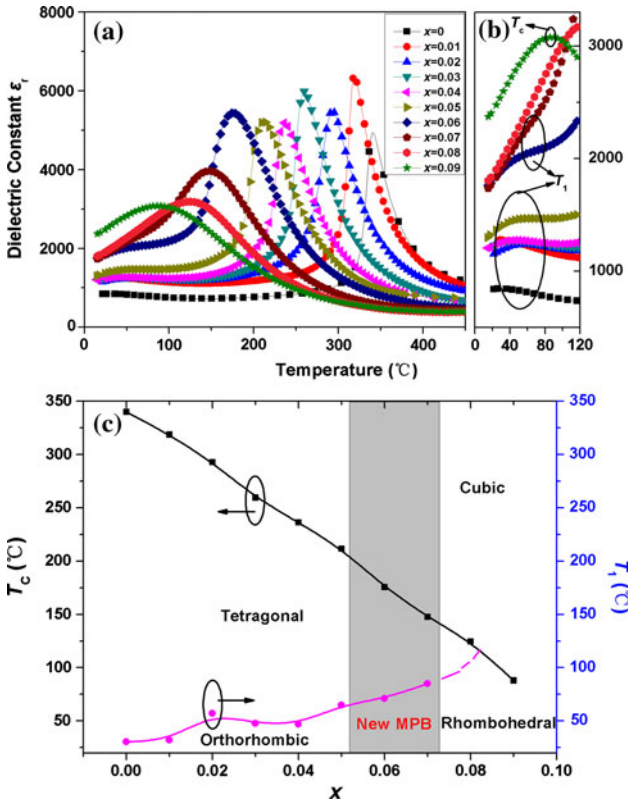

Fig. 2 The temperature dependence of the dielectric constant (ε_r) of the $0.94(K_{0.4-x}Na_{0.6}Ba_xNb_{1-x}Zr_x)O_3$–$0.06LiSbO_3$ ceramics measured at 10 kHz in the temperature range **a** from room temperature to 450 °C, **b** from room temperature to 120 °C, respectively; and **c** the phase diagram for the ceramics

with $x = 0.07$ and its' XRD pattern shows rhombohedral phase at room temperature. As a result, it is suggested that the ferroelectric–ferroelectric phase transition temperature T_1, for the samples with $x = 0.07$, is related to rhombohedral–tetragonal phase transition similar to PZT systems [22]. It is also indicated that the samples with $x = 0.06$ have both rhombohedral–orthorhombic and orthorhombic–tetragonal phase transitions around room temperature. For the compositions with $x = 0.08$–0.09, no dielectric anomaly is observed below T_C, and it is suggested that the symmetry of the samples changed from rhombohedral phase to cubic phase at T_C directly.

Figure 2c shows the phase transition for the $0.94(K_{0.4-x}Na_{0.6}Ba_xNb_{1-x}Zr_x)O_3$–$0.06LiSbO_3$ ceramics based on careful analysis of XRD patterns and temperature dependence of dielectric constant as shown in Figs. 1 and 2a, b, respectively. It can be observed that the T_C decreases almost linearly with a ratio of about −28 °C per 1% mol of $BaZrO_3$. For the compositions with $x = 0$–0.05, the phase transitions are similar to most of the KNN-based ceramics. While, the phase evolutions are from rhombohedral to tetragonal and then to cubic for the ceramics with $x = 0.07$ and directly from rhombohedral to cubic for the samples with $x = 0.08$–0.09 with the increase of temperature. As a result, the compositions with $x \sim 0.06$ may have both rhombohedral–orthorhombic and orthorhombic–tetragonal phase transitions near room temperature. The new MPB or polymorphic phase transition for KNN-based ceramics is different from previously well-studied phase boundary associated with coexistence of orthorhombic and tetragonal phase [4–14, 16, 19].

Figure 3a–d show the SEM micrographs of the ceramics with $x = 0.01$, 0.03, 0.06, and 0.09, and their average grain sizes are 2.01, 2.67, 2.68, and 1.26 μm, respectively. The evolution of average grain sizes with compositions suggests that a low concentration of $BaZrO_3$ ($x = 0.03$) is favorable for the growth of grain, a high $BaZrO_3$ concentration ($x = 0.09$) will lead to grain refinement. The result is owing to the fact that a low concentration of $BaZrO_3$ can well defuse into the KNN lattices to form a new homogeneous solid solution, while, if the x is too high, some of the $BaZrO_3$ particles may exist near the grain boundary thus restrict the growth of the grains. Moreover, the composition with $x = 0.03$ has uniform grain size and low porosity. As shown in Fig. 3e, the density of the ceramics gets the highest value for the composition with $x = 0.03$.

The P–E hysteresis loops for the ceramics are shown in Fig. 4a, and all the compositions show a typical ferroelectric hysteresis loop. The existence of ferroelectric properties for the compositions with $x = 0.07$–0.09 are in well agreement with the rhombohedral symmetry determined via dielectric behaviors and XRD data. The remnant polarization (P_r) and coercive field (E_C) as a function of x are shown in Fig. 4b. It can be found that a low concentration of $BaZrO_3$ with $x = 0.01$–0.02 will lead to the enhancement of ferroelectric property of the ceramics, and the increase of x up to 0.09 will lead to the decrease of P_r. As to E_C of the ceramics, it decreases with x in the whole range considered. The decreasing trend of P_r seems queer near the MPB region, while it is in fact not strange as the high concentration of $BaZrO_3$ will lead to formation of secondary phase as shown in Fig. 1a, and the non-perovskite secondary phase acts as a barrier for long-range ferroelectric interaction.

Figure 5 shows the ε_r as well as the dielectric loss ($\tan\delta$) measured at 1 kHz as a function of x. It can be observed that both the ε_r and $\tan\delta$ have an increasing trend with the increase of $BaZrO_3$ concentration. The increase of $\tan\delta$ with x is mainly attributed to the formation of secondary phase and the deliquescence of the ceramics, while the increase of ε_r is related to the increasing of T_{R-O} besides the decreasing of T_C. The increase of ε_r is of significance for the enhancement of piezoelectric properties as almost all high performance piezoelectric ceramics have large ε_r [18]. However, the ε_r for most of the KNN-based ceramics is rather low near T_{O-T} ($\varepsilon_r \sim 1000$) compared to PZT materials [18].

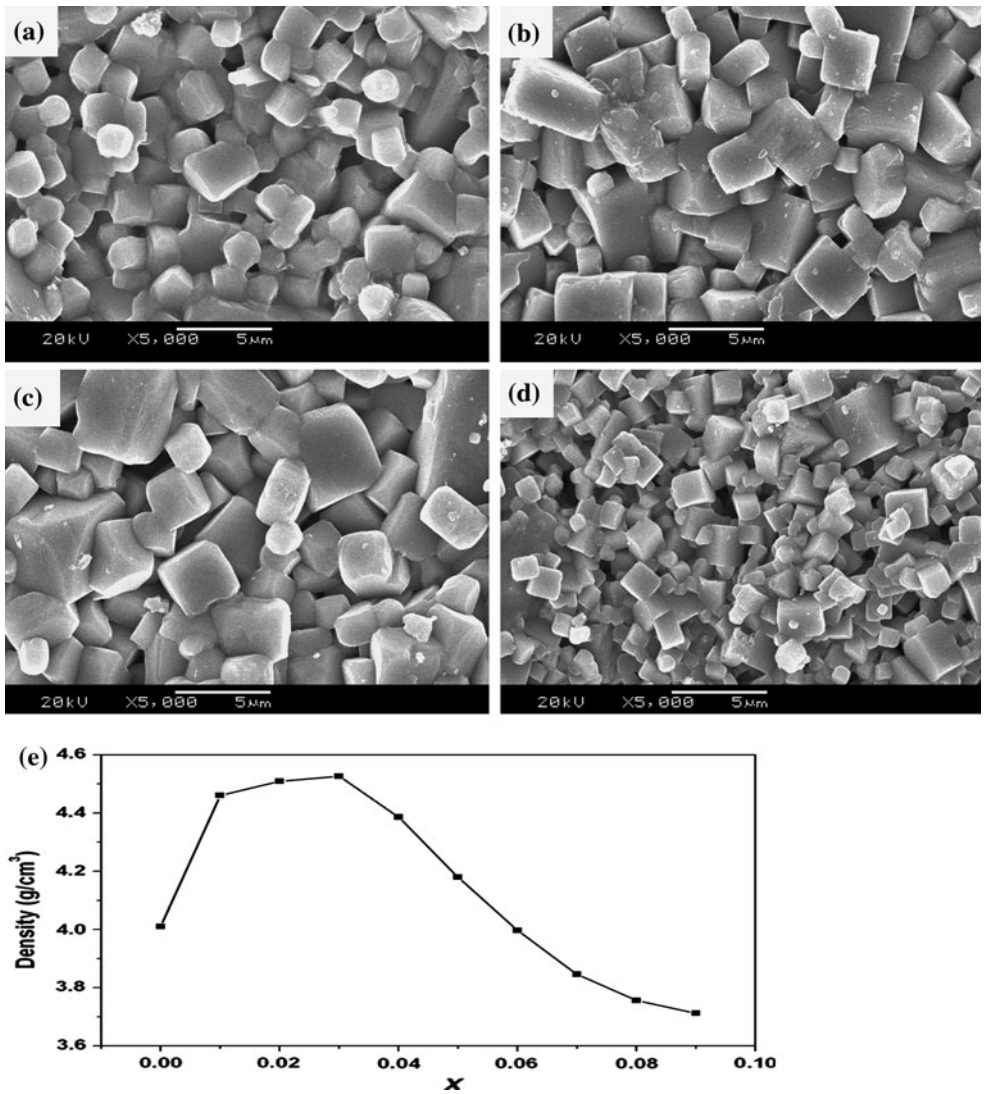

Fig. 3 The SEM image of the $0.94(K_{0.4-x}Na_{0.6}Ba_xNb_{1-x}Zr_x)O_3$–$0.06LiSbO_3$ ceramics with **a** $x = 0.01$, **b** $x = 0.03$, **c** $x = 0.06$, and **d** $x = 0.09$ sintered at 1120 °C; and **e** the density of the ceramics as a function of composition

Both the ε_r and P_r are key parameters related to piezoelectric activity, as the piezoelectric properties of a ferroelectric ceramic can be expressed using the empirical formula [18], piezoelectric coefficient $d_{33} \sim \alpha\varepsilon_r P_r$, where α is parameter with little dependence on composition or temperature. It is worthwhile to compare the empirical result with piezoelectric parameters measured for the understanding of piezoelectric activities.

Figure 6 shows piezoelectric properties (d_{33} and k_P) measured and the $\varepsilon_r P_r$ related to empirical value, as a function of x. It was found that the electromechanical coupling factor k_P could be significantly enhanced by a small amount of $BaZrO_3$ and got the maximum 48.6% for the samples with $x = 0.03$, while further increase of x leads to the decrease of k_P. In comparison with Fig. 3, the uniform and dense microstructure is probably responsible for the enhancement of k_P for the compositions near $x = 0.03$. As to the piezoelectric coefficient, it possesses an increasing trend until $x = 0.06$ with $d_{33} = 344$ pC/N, and the enhancement is attributed to the formation of new MPB, but the k_P is only $k_P = 32.4\%$. The phenomenon that the d_{33} and k_P of the ceramics do not have their maximum value at the same composition is probably due to the formation of secondary phase as shown in Fig. 1a, and the non-perovskite secondary phase formed acts as a barrier in transformation between electrical and mechanical energy. The $\varepsilon_r P_r$ value for the compositions with $x = 0.01$–0.06 is much higher than that for other compositions; thus, it has similar behavior as the experimentally measured value to some extent. As a result, it is suggested the enhancement of piezoelectric properties in the system considered is mainly attributed to the increase of ε_r near the new MPB, while the

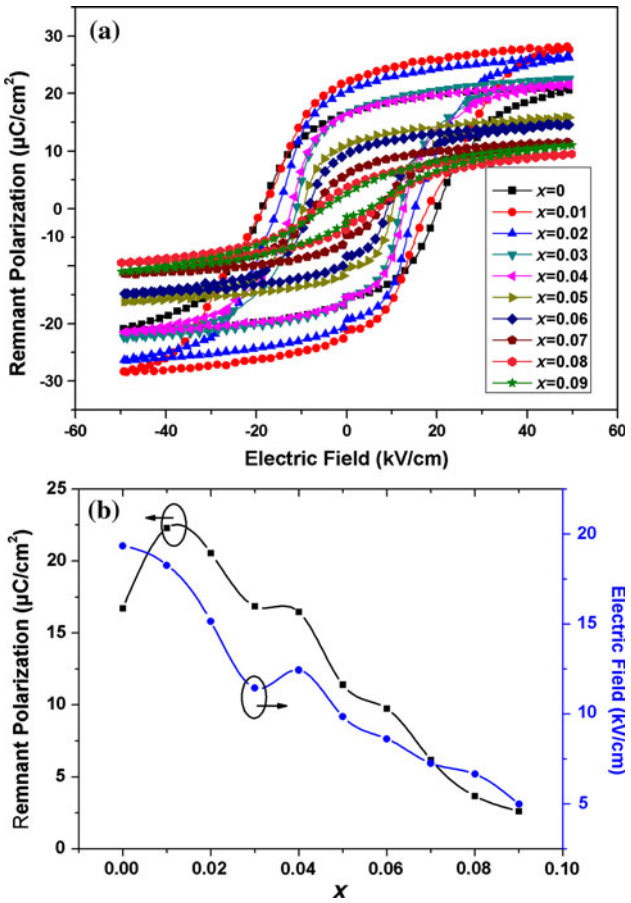

Fig. 4 The *P–E* hysteresis loops for the ceramics (**a**) and the Remnant polarization (P_r) and coercive field (E_C) of the ceramics (**b**)

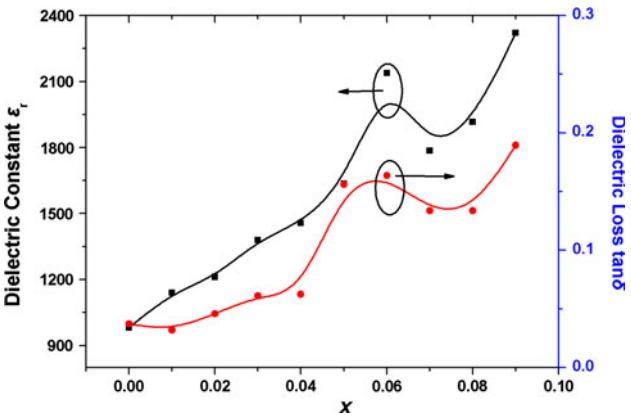

Fig. 5 The dielectric constant (ε_r) and dielectric loss ($\tan\delta$) measured at 1 kHz as a function of x

decrease of P_r possibly acts as a barrier for further enhancement of piezoelectric properties. The construction of such MPB in KNN-based ceramics without decreasing the P_r can possibly further enhance the piezoelectric activity, and it will be the future study for us.

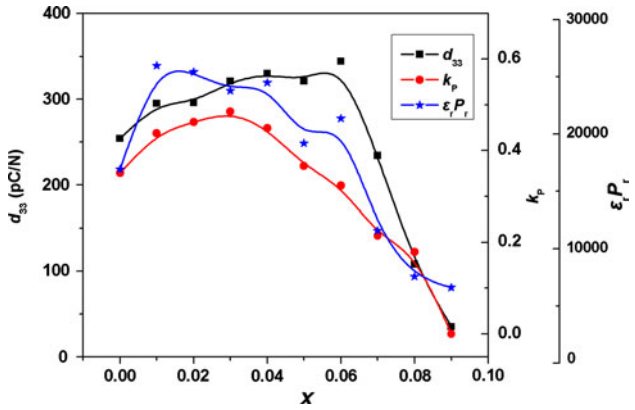

Fig. 6 The piezoelectric coefficient (d_{33}), empirical piezoelectric parameter ($\varepsilon_r P_r$), and electromechanical coupling factor (k_p) of the $0.94(K_{0.4-x}Na_{0.6}Ba_xNb_{1-x}Zr_x)O_3$–$0.06LiSbO_3$ ceramics

Conclusions

In summary, the phase transitions and the properties of the $0.94(K_{0.4-x}Na_{0.6}Ba_xNb_{1-x}Zr_x)O_3$–$0.06LiSbO_3$ ceramics were investigated. It was found that the addition of $BaZrO_3$ changes the symmetry from tetragonal dominant phase for the ceramics with $x = 0$–0.06 to rhombohedral phase for the ceramics with $x = 0.07$–0.09. As a result, a new MPB with both rhombohedral–orthorhombic and orthorhombic–tetragonal phase transitions near room temperature was constructed, and the enhanced piezoelectric properties ($d_{33} = 344$ pC/N and $k_P = 32.4\%$ with $x = 0.06$) were obtained. The enhancement of piezoelectric properties in the system is mainly attributed to the increase of ε_r near the new MPB, while the formation of secondary phase leads to the decrease of P_r and acts as a barrier for further enhancement of piezoelectric properties. The results suggest that further enhancement of the piezoelectric properties can be obtained by construction of such a new MPB in KNN-based ceramics.

Acknowledgement This study was supported by National Science Foundation of China (NSFC Nos. 50772068 and 50972095) and Foundation of Doctor Training Program in University and College in China (Nos. 20030610035 and 20080610020).

References

1. Saito Y, Takkao H, Tani T, Nonoyama T, Takatori K, Hommal T, Nagaya T, Nakamura M (2004) Nature 84:432
2. Xiao DQ, Wu JG, Wu L, Zhu JG, Yu P, Lin DM, Liao YW, Sun Y (2009) J Mater Sci 44:5408. doi:10.1007/s10853-009-3543-3
3. Rödel J, Jo W, Seifert KTP, Anton EM, Granzow T (2009) J Am Ceram Soc 92:1153
4. Akdogan EK, Kerman K, Abazari M, Safari A (2008) Appl Phys Lett 92:112908
5. Tanaka D, Tsukada T, Furukawa M, Wada S, Kuroiwa Y (2009) Jpn J Appl Phys 48:09KD08

6. Guo YP, Kakimoto K, Ohsato H (2004) Appl Phys Lett 85:4121
7. Park HY, Ahn CW, Song HC, Lee JH, Nahm S, Uchino K, Lee HG, Lee HJ (2006) Appl Phys Lett 89:062906
8. Lei C, Ye ZG (2008) Appl Phys Lett 93:042901
9. Lin DM, Kwok KW, Chan HLW (2007) J Appl Phys 102:034102
10. Sun XY, Chen J, Yu RB, Sun C, Liu GR, Xing XR, Qiao LJ (2009) J Am Ceram Soc 92:130
11. Wang R, Xie RJ, Hanada K, Matsusaki K, Kawanaka H, Bando H, Sekiya T, Itoh M (2008) J Electroceram 21:263
12. Wu JG, Wang YY, Xiao DQ, Zhu JG, Pu ZH (2007) Appl Phys Lett 91:132914
13. Zhang SJ, Xia R, Shrout TR (2007) Appl Phys Lett 91:132913
14. Zuo RZ, Fang XS, Ye C (2007) Appl Phys Lett 90:092904
15. Wang RP, Bando H, Katsumata T, Inaguma Y, Taniguchi H, Itoh M (2009) Phys Status Solidi RRL 3:142
16. Wu JG, Xiao DQ, Wang YY, Zhu JG, Yu P (2008) J Appl Phys 103:024102
17. Zuo RZ, Fu J, Lv DY, Liu Y (2010) J Am Ceram Soc 93:2783
18. Zhang SJ, Xia R, Shrout TR (2007) J Electroceram 19:251
19. Yang W, Jin DR, Wang TT, Cheng JR (2010) Physica B 405:1918
20. Lee T, Kwok KW, Chan HLW (2008) J Phys D Appl Phys 41:155402
21. Liu WF, Ren XB (2009) Phys Rev Lett 103:257602
22. Cox DE, Noheda B, Shirane G, Uesu Y, Fujishiro K, Yamada Y (2001) Appl Phys Lett 79:400